

# Rotational Motions Excited by Vertical Harmonic Motions

Tadokoro Chiharu<sup>1\*</sup>, Kadowaki Kei<sup>1</sup>, Mori Hiroki<sup>2</sup>, Nagamine Takuo<sup>1</sup>

1. Department of Mechanical Engineering, Saitama University, Saitama 338-8570, Japan;

2. Department of Mechanical Engineering, Kyushu University, Fukuoka 819-0395, Japan

(Received 18 October 2017; revised 20 December 2017; accepted 5 January 2018)

**Abstract:** Rotation of a pair of wings was driven by the vertical harmonic motion of a pin inserted into the center hole of the wings. To elucidate the mechanism by which the rotational motion of the wings was excited, the relationship between the wings and the pin was examined by tracking their motions using both displacement measurements and high-speed photography. The motion modes occurred in this study were categorized into five types: slipping, rolling, jumping (without eccentricity), jumping (with eccentricity), and non-rotation. In the case that the hole of the wings was located at a distance from the center of the wings, referred to as "with eccentricity," the slipping, jumping (with eccentricity), and non-rotation modes resulted. The experimental results showed that the mechanism of the jumping (with eccentricity) was different from that of the other modes (slipping, rolling, jumping (without eccentricity)), which are well known to be driven by the periodical reaction of the wings against the vertical vibration of the pin. It was found that the jumping (with eccentricity) was driven by the non-periodical force with the collision between the wing hole and the pin.

**Key words:** motion transformation; rotation; vibration; hula-hoop

**CLC number:** TN925      **Document code:** A      **Article ID:** 1005-1120(2018)01-0051-07

## 0 Introduction

The rotational motion excited by vibrations has been utilized to develop novel rotational devices that can be employed in place of electric motors. For example, rotary motors utilizing ultrasonic vibration are currently commercially available. The advantages of these rotary motors using ultrasonic vibration are high torque and high efficiency at low speeds<sup>[1]</sup>.

Several configurations for the rotational motions excited by the sonic-range vibrations have been examined. Mainly, there are two configurations of rotational axis and vibration direction, parallel configuration<sup>[2-4]</sup> and perpendicular configuration<sup>[5-10]</sup>. As for parallel configuration, Nakano et al.<sup>[3]</sup> examined a motion transformation mechanism from oscillation to rotation experimentally and numerically, and Sato et al.<sup>[4]</sup> pro-

posed the energy regeneration from vibration by an oscillatory rotor. As for perpendicular configuration, automatic balancer<sup>[5]</sup>, gari-gari dragonfly<sup>[6-7]</sup>, and hula-hoop<sup>[8-10]</sup> have been examined. Gari-gari dragonfly is a Japanese traditional toy, which is that a propeller can be rotated by vertical harmonic motions of a pin inserted into the center hole of the propeller. This rotational motion looks similar to the motion of a hula-hoop. The rotational motion of the hula-hoop is well-known to be driven by the periodical reaction of the hula-hoop against a gymnast's waist. Caughey<sup>[8]</sup> proposed a model considered the periodic motion of the athlete's waist along one axis, which is same as the model of parametric resonance<sup>[11-13]</sup>, and found that the pendulum rotation with an average angular velocity equal to the excitation frequency. Belyakov and Seyranian<sup>[9]</sup> proposed a model considered the excitation along two axes correspond-

\* Corresponding author, E-mail address: tadokoro@mail.saitama-u.ac.jp.

ing to an elliptic trajectory of the motion of the athlete's waist and obtained the solutions by the averaging method<sup>[14]</sup> corresponding to the rotation with a constant angular velocity equal to the excitation frequency. Also, Seyranian and Belyakov<sup>[10]</sup> proposed approximate analytical solutions. In the above-mentioned models, it is assumed that the rotation of the hula-hoop is driven by the periodical reaction of the hula-hoop against the periodical motion of the gymnast's waist. However, the rotational motion driven by non-periodical reaction has received little attention. Here, using an apparatus of the similar configuration to the gari-gari dragonfly, the rotational motion driven by non-periodical reaction of the propeller against the pin occurred. To examine the generation conditions and the mechanism of the rotational motion excited by vertical motion, the relationship between the propeller wing and the inserted pin was examined by tracking their relative motions.

## 1 Experiment

### 1.1 Apparatus

Fig. 1 shows the schematic diagram of the apparatus used in this study. The main part of the apparatus consisted of a wing (acrylic, size 20 mm×100 mm×1 mm, mass 3 g), a pin (diameter 1 mm), and a vibration exciter. The wing had a hole in its center (diameter,  $\varphi$ , of 2 or 7 mm) as shown in Fig. 2. The distance,  $e$ , between the centers of the hole and the wing was either 0 or 10 mm. Four marks for analyzing the motion of the wing were made in the wing. The pin was inserted into the hole in the wing.

The end of the pin was bent into an L-shape so as not to drop the wing. The pin was mounted on a block (wood, size 10 mm×10 mm×10 mm), which was placed atop the vibration exciter. The wing was rotated by the vertical harmonic motion of the pin. The amplitude,  $A$ , and the frequency,  $f_v$ , of the vertical harmonic motion of the pin were adjusted by a function generator. The vibration frequency,  $f_v$ , of the pin and

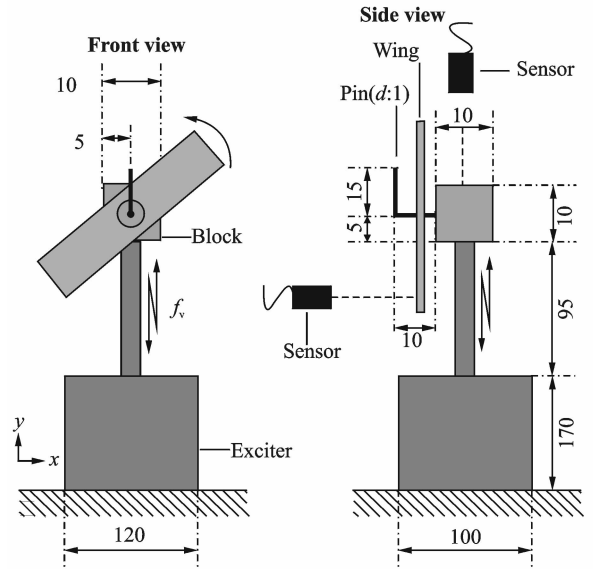


Fig. 1 Schematic of apparatus (unit: mm)

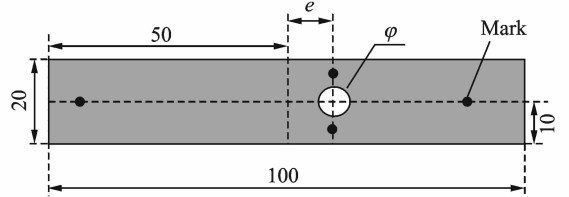


Fig. 2 Specifications of wing (unit: mm)

the rotational frequency,  $f_r$ , of the wing were evaluated by two separate displacement sensors. The phase difference between the pin and the wing were measured by a high-speed camera and motion analysis software.

### 1.2 Procedure

The wing was installed on the pin and was rotated by means of the vertical harmonic motion of the pin. The rotational frequency of the wing was measured at values of  $e=0$  and 10 mm,  $\varphi=2$  and 7 mm,  $A=1.0$  and 1.5 mm, and  $f_v=5-45$  Hz. Additionally, the motion of the pin and the wing was captured by a high-speed camera, and the centers of the wing and the pin were tracked by motion analysis software, where the position of the wing's center of gravity was calculated by the position of the four marks.

## 2 Results

### 2.1 Effect of $f_v$ on $f_r$

The motion modes observed during the

measurements of  $f_r$  and  $f_v$ , were of four types: Slipping, rolling, jumping, and non-rotation. The slipping mode is that the wing was rotated with  $f_r = f_v$ . The rolling mode is that the wing was rotated with  $f_r < f_v$  and the wing hole was kept in continuous contact with the pin. The jumping mode is that the wing was rotated with  $f_r < f_v$  and the wing hole allowed to jump against the pin. The non-rotation mode is that the wing was not rotated while the pin was vibrated at  $f_v$ .

Fig. 3 shows the effect of the vertical harmonic motion frequency,  $f_v$ , of the pin on the rotational frequency,  $f_r$ , of the wing at  $e=0$  mm,  $\varphi=7$  mm, and  $A=1.5$  mm. In the cases where  $e=0$  mm, the placement of the hole of the wing corresponded to the center of the wing. When  $f_v < 15$  Hz, the wing was not rotated by the vertical harmonic motion of the pin. When  $f_v > 15$  Hz and the initial rotational speed of the wing was low, the jumping mode of motion occurred. The value of  $f_r$  in the jumping mode increased qualitatively with increasing  $f_v$ . The jumping mode occasionally shifted into the rolling mode. However, the rolling mode did not shift back to the jumping mode. The value of  $f_r$  in the rolling mode increased linearly with increasing  $f_v$ . The solid line shows the linear trendline fit to the data:  $f_r = a f_v$ , where  $a = 0.86$  ( $R^2 = 1.00$ ). When the pin was vibrated through one cycle, the wing rotated  $360^\circ$  around the pin with a rolling contact. The rotational speed,  $v$ , is described by  $v = \pi \varphi f_r$ . The circumference,  $L$ , of the trajectory of the wing's center is  $L = \pi(\varphi - d)$ . The period,  $T$ , of one cycle of the pin is  $T = 1/f_v = L/v = (\varphi - d)/\varphi f_r$ . Therefore, the relationship between  $f_r$  and  $f_v$  is  $f_r = (1 - d/\varphi) f_v$ . When  $d = 1$  mm and  $\varphi = 7$  mm, the resulting relationship is  $f_r = 6/7 f_v = 0.86 f_v$ , which corresponds to the experimental results.

Fig. 4 shows the effect of the vertical harmonic motion frequency of the pin,  $f_v$ , on the rotational frequency of the wing,  $f_r$ , at  $e=10$  mm,  $\varphi=7$  mm, and  $A=1.5$  mm. In the case where

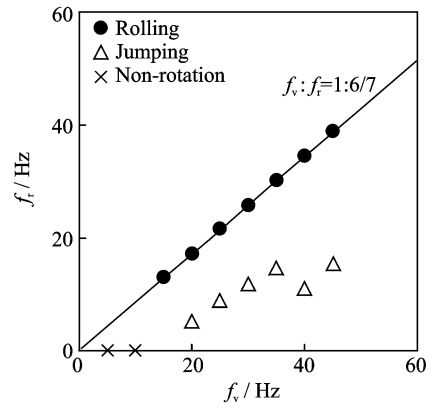


Fig. 3 Effect of  $f_v$  on  $f_r$  at  $e=0$  mm,  $\varphi=7$  mm, and  $A=1.5$  mm (solid line: Linear trendline)

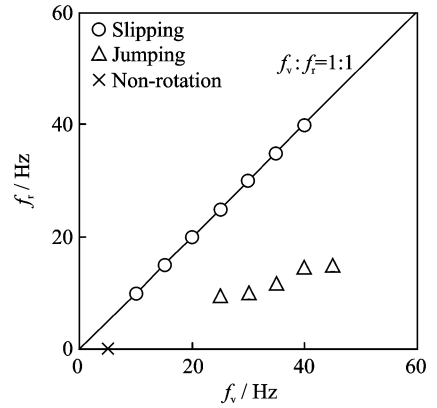


Fig. 4 Effect of  $f_v$  on  $f_r$  at  $e=10$  mm,  $\varphi=7$  mm, and  $A=1.5$  mm (solid line: Linear trendline)

$e=10$  mm, the hole of the wing is located at a distance of 10 mm from the center of the wing. When  $f_v < 10$  Hz, the wing was not rotated by the vertical harmonic motion of the pin. When  $f_v > 20$  Hz and the initial rotational speed of the wing was low, the jumping mode occurred but did not shift to any other motion modes. When  $f_v \geq 10$  Hz and the initial rotational speed of the wing was sufficiently high, the slipping mode occurred. The value of  $f_r$  in the slipping mode increased linearly with increasing  $f_v$ . The solid line shows the linear trendline fit to the data:  $f_r = a f_v$ , where  $a = 1.00$  ( $R^2 = 1.00$ ).

## 2.2 Trajectory of wing motion

Fig. 5 shows the temporal change in wing displacement of the wing's center of gravity along the  $y$ -axis (left) and the trajectory of wing's center of gravity in the  $x$ - $y$  plane (right) under each

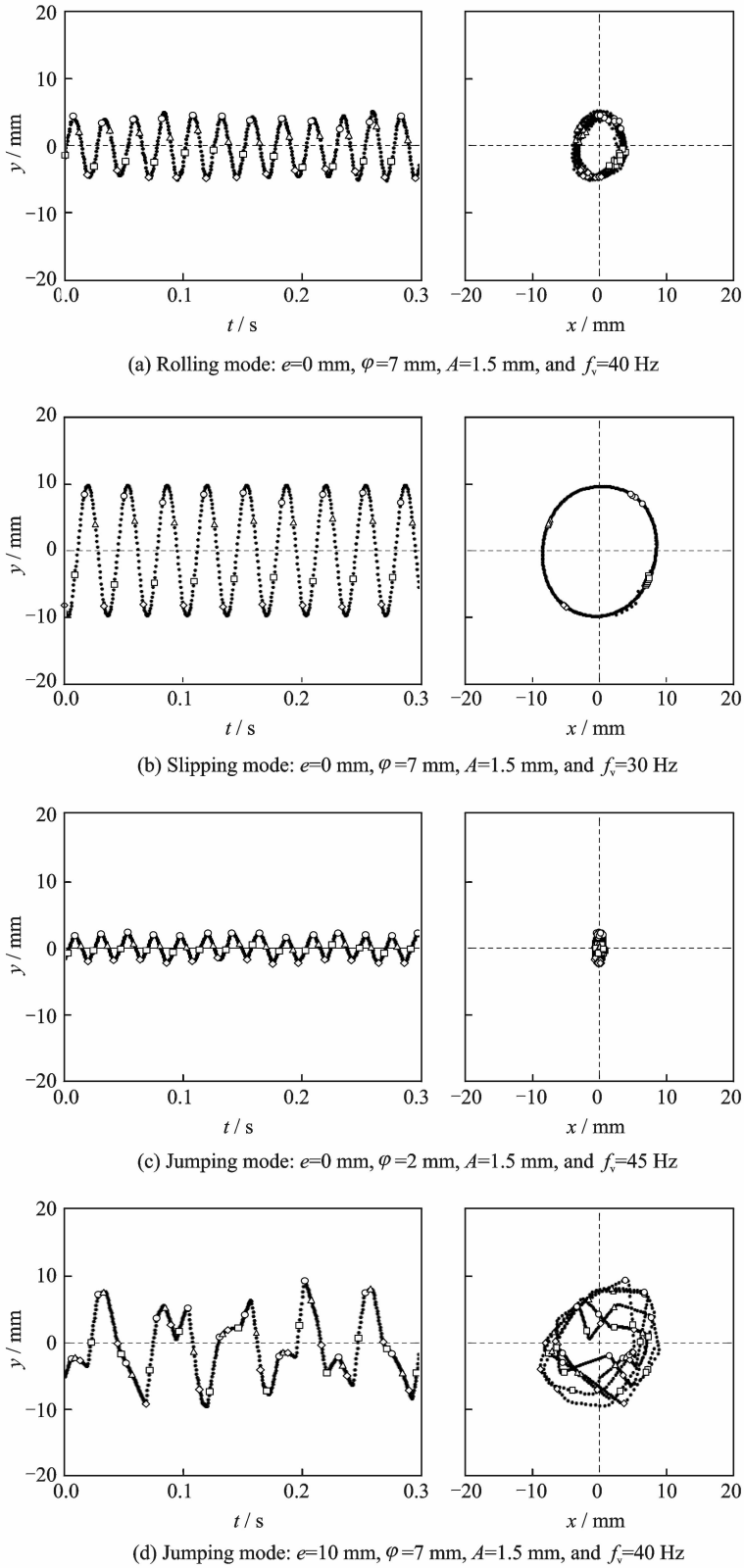


Fig. 5 Temporal change in displacement of the wing's center of gravity along the  $y$ -axis (left) and trajectory of the wing's center of gravity in the  $x$ - $y$  plane (right).

mode of motion. In Fig. 5, the closed circle symbols represent the position of the wing's center of gravity as calculated by the position of the four marks in the wing. The open circle, diamond,

square, and triangle symbols represent the points in time when the pin is located at particular positions in the vertical harmonic motion cycle: the top dead point, the bottom dead point, the mid-

dle point (upward), and the middle point (downward), respectively.

In both the rolling mode and the slipping mode, the trajectory of the wing motion was elliptical in shape. The frequency ( $f_y$ ) of the  $y$ -axis motion of the wing was same as the frequency ( $f_v$ ) of the vertical harmonic motion of the pin. However, the  $y$ -axis motion of the wing lagged behind that of the pin. The phase difference in the slipping mode was larger than that in the rolling mode.

In the jumping mode, two different wing motion trajectories occurred. When  $e=0$  mm, the trajectory looked elliptical. The  $y$ -axis motion of the wing was equivalent to that of the pin in both frequency and phase. In contrast, when  $e=10$  mm, the wing trajectory exhibited irregular pattern. The relationship of both the frequency and the phase between the motion of wing and the

pin was not readily apparent.

Therefore, these results imply that the mechanism of the wing rotation in the jumping mode is different with and without eccentricity.

Temporal change in displacement of the wing along the  $y$ -axis (left) and trajectory of wing motion in the  $x$ - $y$  plane (right). The open circle, diamond, square, and triangle symbols represent the times when the position of the pin in the cycle of vertical harmonic motion is at the top dead point, bottom dead point, middle point (upward), and middle point (downward), respectively.

### 2.3 Phase difference between wing and pin

Fig. 6 shows the effect of the vertical harmonic motion frequency ( $f_v$ ) of the pin on the phase difference ( $\theta$ ) of the  $y$ -axis wing motion in relation to the vertical harmonic motion of the pin, which was calculated by  $2\pi\tau/T_v$ , where  $\tau$  and  $T_v$  are a period from the wing's top dead posi-

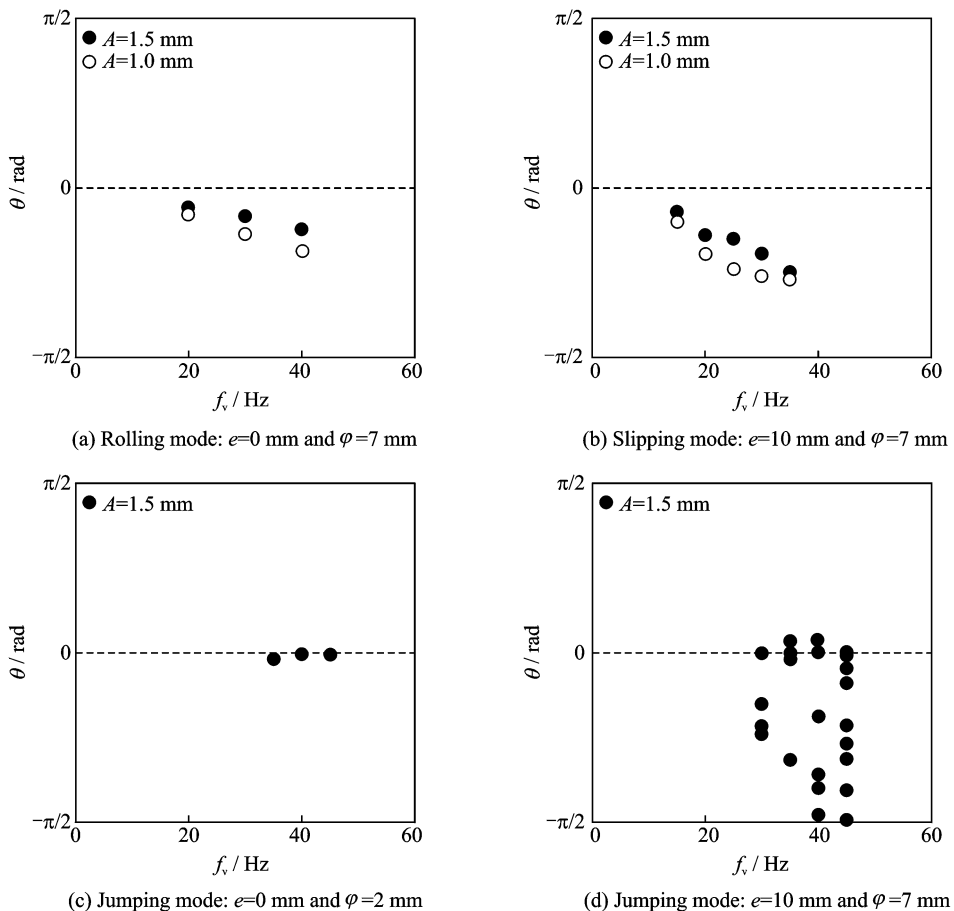


Fig. 6 Effect of  $f_v$  on the phase difference ( $\theta$ ) of  $y$ -axis wing motion in relation to the vertical harmonic motion of the pin

tion to the pin's top dead position as shown in Fig. 5 and a period of the vertical harmonic motion of the pin, respectively. In the rolling mode and the slipping mode, the phase difference ( $\theta$ ) had a negative value, which increased with increasing frequency of the pin vertical harmonic motion ( $f_v$ ). The qualitative change in  $\theta$  was largely independent of the amplitude ( $A$ ) of the vertical harmonic motion of the pin. In the jumping mode without eccentricity ( $e = 0$  mm), the values of  $\theta$  were approximately zero and did not change with  $f_v$ . In the jumping mode with eccentricity ( $e = 10$  mm), the values of  $\theta$  varied inconsistently with  $f_v$ .

### 3 Discussion

#### 3.1 Characteristics of rotation mode

Five distinct motion modes occurred in this study: Slipping, rolling, jumping (without eccentricity), jumping (with eccentricity), and non-rotation. The relationship between  $f_r$  and  $f_v$  and the relationship between  $f_y$  and  $f_v$  for each mode is summarized in Table 1.

**Table 1** Characteristics of rotation mode

Rotation mode (wing type)	$f_r$ versus $f_v$	$f_y$ versus $f_v$
Rolling (without eccentricity)	$f_r = (1 - d/\phi)f_v$	$f_y = f_v$
Slipping (with eccentricity)	$f_r = f_v$	$f_y = f_v$
Jumping (without eccentricity)	$f_r \neq f_v$	$f_y = f_v$
Jumping (with eccentricity)	$f_r \neq f_v$	$f_y \neq f_v$
Non-rotation		

#### 3.2 Rotational mechanism of jumping (with eccentricity)

The rotation motion excited by vertical vibration is considered as forced vibration<sup>[2]</sup>. In a system of forced vibration, the reaction of the object lags a constant phase behind the forced displacement. It means that the energy of forced displacement translates to the object motion. The results of phase difference shown in Fig. 6 show that slipping, rolling, and jumping (without eccentricity) are well-known mode, which are driven by the

periodical reaction of the wing against the periodical motion of the pin such as forced vibration.

In the jumping mode (with eccentricity), the values of  $\theta$  varied inconsistently with  $f_v$  as shown in Fig. 6(d). It was observed that sometimes the motion of the wing was ahead of the motion of the pin. It means that the motion of the pin brakes the motion of the wing. The rotation mechanism in jumping mode (with eccentricity) is different from simple forced-vibration. The observation results imply that the rotational motion of the wing was driven by the non-periodical force with the collision between the wing hole and the pin.

### 4 Conclusions

The relationship between the wing and the pin was examined experimentally by tracking their respective motions. Here, five distinct motion modes occurred: slipping, rolling, jumping (without eccentricity), jumping (with eccentricity), and non-rotation. In the case where the hole of the wing was located at a distance from the center of the wing, jumping mode (with eccentricity) occurred. In jumping mode (with eccentricity), the phase difference between  $f_y$  and  $f_v$  varied inconsistently. The rotational motion of the wing was driven by the non-periodical force with the collision between the wing hole and the pin.

#### References:

- [1] UEHA S. Rotary ultrasonic motors[J]. The Journal of the Acoustical Society of Japan, 1988, 44(7): 519-524.
- [2] WALKER G T. On a dynamical top[J]. Quarterly Journal of Pure and Applied Mathematics, 1896.
- [3] NAKANO K, SATO Y, GOTO K, et al. A motion transformation mechanism from oscillation to rotation[J]. Transactions of the Japan Society of Mechanical Engineers Series C, 2000, 66: 9-15.
- [4] SATO Y, NAGAMINE T, ANDO Y. Study on energy conversion from vibrational to rotational energy by an oscillatory rotor[J]. Transactions of the Japan Society of Mechanical Engineers Series C, 2005, 71: 2850-2856.
- [5] BLEKHMANN I I. Synchronization in science and

- technology[M]. American Society of Mechanical Engineers, 1988.
- [6] OTA H, HANDA T. Research on rotation of a rotor in gari-gari dragonfly (1st report, experiments on rotating direction of a rotor) [J]. Bulletin of Aichi University of Technology, 2010, 7: 1-6.
- [7] OTA H, HANDA T, KABEYA T. Research on rotation of a rotor in gari-gari dragonfly (2st report, Theoretical Consideration on rotation of a rotor) [J]. Bulletin of Aichi University of Technology, 2010, 7: 7-14.
- [8] CAUGHEY T K. Hula-hoop; An example of hetero-parametric excitation[J]. American Journal of Physics, 1960, 28(2): 104-109.
- [9] BELYAKOV A O, SEYRANIAN A P. The hula-hoop problem[J]. Doklady Physics, 2010, 55(2): 99-104.
- [10] SEYRANIAN A P, BELYAKOV A O. How to twirl a hula hoop[J]. American Journal of Physics, 2011, 79(7): 712-715.
- [11] LANDAU L D, LIFSHITZ E M. Mechanics, vol. 1 [M]. Course of Theoretical Physics 3, 1976.
- [12] PIKOVSKY A, ROSENBLUM M, KURTHS J. Synchronization: A universal concept in nonlinear sciences[M]. Cambridge University Press, 2003.
- [13] NAYFEH A H, MOOK D T. Nonlinear oscillations [M]. John Wiley & Sons, 2008.
- [14] NAYFEH A H. Introduction to perturbation techniques[M]. John Wiley & Sons, 2011.

Dr. **Tadokoro Chiharu** received the Ph. D. degree in Mechanical Engineering from Yokohama National University, Yokohama, Japan, in 2014. From 2014 to 2016, he joined in Tokyo University of Science, Tokyo, Japan, where he was an assistant professor in the Department of Mechanical Engineering. From 2016, he works as an assistant professor in Saitama University, Saitama, Japan.

Mr. **Kadowaki Kei** received the Master degree of Mechanical Engineering from Saitama University, Saitama, Japan, in 2017. From 2017, he works in FURUKAWA CO., LTD., Japan.

Dr. **Mori Hiroki** received the Ph. D. degree in Mechanical Engineering from Kyushu University, Fukuoka, Japan, in 2007. From 2007 to 2014, he joined in Saitama University, Saitama, Japan, where he was an assistant professor. From 2014 to present, he joined in Kyushu University, Fukuoka, Japan, where he is an associate professor.

Prof. **Nagamine Takuo** received the Ph. D. degree in Mechanical Engineering from Saitama University, Saitama, Japan, in 2005. From 2000 to present, he has been with Saitama University, Saitama, Japan, where he is currently a full professor.

(Production Editor: Zhang Bei)